

Estimation of Aliasing Effects Due to Periodical Nonuniform Individual Sampling in High- Q Switched-Capacitor Filters

David Hernandez-Garduno, *Student Member, IEEE*, Jose Silva-Martinez, and José L. Ausín

Abstract—The periodical nonuniform individual sampling scheme has been shown suitable for capacitance spread and total capacitor area reduction in high quality (Q) factor switched-capacitor (SC) filters. However, the use of periodical nonuniform clock signals results in additional aliasing components in the output spectrum. This paper presents a simple model to analyze the generation of such alias components and gives practical expressions to estimate their power. The results are verified through circuit simulation of a 10.7-MHz second-order SC bandpass filter in a 0.35- μm CMOS technology. Implications on the use of this technique in the design of intermediate-frequency filters are discussed.

Index Terms—High- Q , intermediate-frequency (IF) filters, periodical nonuniform individual sampling, switched-capacitor (SC) filters, SC networks.

I. INTRODUCTION

SWITCHED-CAPACITOR (SC) filtering techniques are routinely used in baseband applications due to their inherent properties such as accuracy, robustness, and compatibility with CMOS technologies. The traditional SC techniques are, however, not quite efficient for the realization of high- Q filters due to the need of large capacitive spread. This issue is more relevant in submicrometer digital technologies where the lack of dedicated poly layers limits the designer to the use of low-density metal-metal capacitors. Hence, there is a need for reduced capacitive spread design techniques for highly selective filters compatible with CMOS digital technologies.

A typical single-ended switched-capacitor (SC) biquadratic bandpass filter is shown in Fig. 1. Let us consider, initially, that the operating clock phases of the SC C_3 (θ_1 and θ_2) coincide with the non-overlapping clock phases of the other SC branches ϕ_1 and ϕ_2 , derived from a master clock ϕ having a period $T_s = 1/f_s$. In this case, the sampling frequency f_s and the capacitor ratios C_4/C_2 , C_4/C_3 , and C_1/C_3 determine the filter's center frequency, the quality factor (Q), and the peak gain, respectively. In particular, for high- Q factors, it can be demonstrated that Q is mainly determined by C_4/C_3 . Since the min-

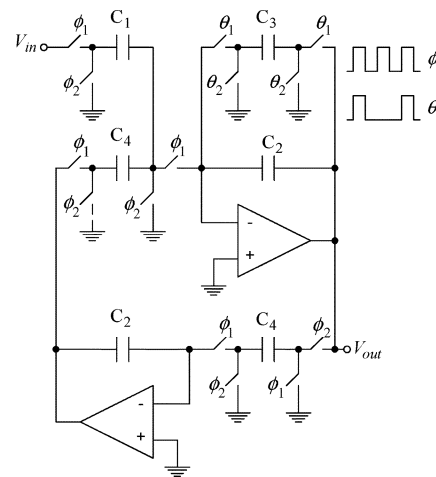


Fig. 1. SC biquadratic bandpass filter.

imum capacitance value for C_3 is limited by kT/C noise and mismatch considerations, high- Q filters lead to a large spread of capacitor values and, hence, impractical values for C_4 may result. As an example, the sixth-order ladder bandpass filter reported in [1] (center frequency = 10.7 MHz, bandwidth = 400 kHz, ripple = 1 dB, clock frequency = 62.5 MHz) requires a maximum capacitive spread of $C_4/C_3 = 32$, leading to a total capacitance of $782 C_u$, where C_u is the unit capacitance; with C_u limited to 0.25 pF, a total capacitance of around 200 pF is needed. To overcome this limitation, T-networks [2], charge recombination techniques [3] and periodical nonuniform individual sampling (PNIS) [4] have been previously proposed. While the first approach [2] increases the input-referred noise and sensitivity to process variations and parasitic capacitors, the technique proposed in [3] uses the amplifiers operating during both phases, requiring faster amplifiers and reducing the filter's flexibility.

Multiple clock solutions have been identified as efficient and flexible techniques for the design of high-performance circuits with relaxed silicon area cost. A couple of examples are the multipath approach commonly used to reduce amplifier count in high-order high-selectivity transfer functions by using lower order circuits [5] and the time-multiplexed topologies used in filter's bank applications [6]. Similarly, by using auxiliary clocks, PNIS allows reducing drastically the capacitive spread, which in turn decreases the overall capacitance needed when high- Q filters are required. The robustness of the filter is not sacrificed since the frequency of the auxiliary clocks is the result of digital operations on the master clock. The main

Manuscript received September 4, 2006; revised November 29, 2006. This paper was recommended by Associate Editor G. Palumbo.

D. Hernandez-Garduno and J. Silva-Martinez are with the Analog and Mixed-Signal Center, Department of Electrical and Computer Engineering, Texas A&M University, College Station, TX 77843-3128 USA (e-mail: davidh@ece.tamu.edu; jsilva@ece.tamu.edu).

J. L. Ausín is in the Department of Electronics and Electrical Engineering, University of Extremadura, 06071 Badajoz, Spain (e-mail: jlausin@unex.es).

Digital Object Identifier 10.1109/TCSII.2006.890403

drawback of this technique is the generation of additional alias components due to the use of slower clocks. Although this is a major issue, it is worth mentioning that SC networks are preceded by a continuous-time anti-alias filter that drastically attenuates the frequency components beyond $f_s/2$, and in the case of intermediate-frequency (IF) filters, reduces the impact of the image sidebands generated by PNIS if located above $f_s/2$. It is, however, mandatory to evaluate the power of the alias generated by PNIS, particularly if it falls below $f_s/2$, and devise a design approach to minimize its impact. A practical method for the prediction of the amount of in-band alias components is the aim of this paper.

The analysis method for PNIS networks is presented in Section II; although an approximation, it allows us to estimate the aliasing effects, and helps in predicting the required stop-band attenuation of the precedent sections to achieve the required specifications. Section III presents simulation results to verify the proposed model and approach for the analysis of the alias components. Section IV follows with implications on the design of intermediate frequency filters using PNIS. Conclusions are given in the last section.

II. ANALYSIS AND ESTIMATION OF ALIASING EFFECTS

The basic idea behind the PNIS scheme consists in a time-averaged control of the effective rate of charge delivered by any given SC structure [4]. In this technique, any individual SC structure is active during m clock periods over a given number N of cycles ($1 \leq m \leq N$) of the master clock signal ϕ . In this way, the equivalent resistance of each SC branch in a circuit is individually controlled by programming the number of clock pulses m . By individually controlling a particular SC branch with a secondary clock, PNIS can modify the filter's gain and Q -factor.

Notice that PNIS technique differs from [7], where a single nonuniform main clock is applied to all SC branches to shift the frequency response of the entire SC filter; therefore filter's parameters that depend on the sampling frequency (i.e., center frequency) can be programmed while Q -factor and peak gain are not affected since they rely on ratio of capacitors and remain unchanged.

In order to illustrate the PNIS feature, let us now consider that the operating clock phases of the SC C_3 are generated from a periodical nonuniform clock signal θ (i.e., θ_1 and θ_2 , $m = 1$, and $N = 2$ in Fig. 1). The SC branch C_3 is only active during m clock periods over a given number N of the master clock ϕ . The equivalent resistance of the SC C_3 is approximately equal to $(NT_s)/(mC_3)$. With such a clock scheme, the equivalent filter's Q -factor is given by $Q \approx (NC_4)/(mC_3)$. Therefore, for the implementation of a given Q -factor value, the required capacitance spread C_4/C_3 is now reduced to $Q \cdot (m/N)$. For high Q -factors, $m = 1$ and $N > 1$ is chosen to obtain the maximum Q with the smallest capacitance spread. By using PNIS with $m = 1$ and $N = 4$, the capacitance in [1] was reduced from 782 C_u down to 219 C_u .

Unfortunately, as a consequence of the larger repetition period of the slower clock signal θ , additional alias components appear at integer multiples of f_s/N that may limit the filter's performance and increase the requirements on the anti-alias

filter that precedes the SC network. This issue is similar to the case of N -path narrowband filters where the effective speed of the clock is reduced by $1/N$ [8], [9], but undesired alias components appear at integer multiples of f_s/N due to mismatch between the N filter paths. While exact expressions to obtain the power of the alias components in PNIS could in principle be derived using polyphase analysis [4], the complexity rapidly increases with the filter's order and number of clock phases used. Instead, we can analyze the generation of such alias components and derive practical expressions to estimate their power using a simple and intuitive alias model that can be used for complex structures. Although an approximation, the method allows us to predict with reasonable accuracy the amount of alias components and gives some insight on how to minimize them.

An equivalent representation of the lossy SC integrator section operating with PNIS is illustrated in Fig. 2. The master clock signal ϕ is again used to generate the non-overlapping clock phases ϕ_1 and ϕ_2 , whereas the operating clock phases of the SC C_3 used in Fig. 1, θ_1 and θ_2 , are modeled by means of an ideal multiplier and a square wave $P(t)$, which represent a switch that is closed when $P(t) = 1$ and opened when $P(t) = 0$. In other words, this model is derived from the fact that the auxiliary clock signal θ can be obtained by masking the master clock signal ϕ with the train of unity pulses $P(t)$. Notice that the branch C_3 is now operating at the sampling frequency f_s and the multiplier modulates the integrator's output with the signal $P(t)$, whose effective sampling frequency f'_s is equal to $f'_s = f_s/N$; for $m = 1$; f'_s has a duty cycle of $(100/N)\%$.

Expressing the signal $P(t)$ in its Fourier series expansion, we have¹

$$P(t) = \frac{1}{N} + \sum_{n=1}^{\infty} b_n \cos\left(\frac{2(2n-1)\pi}{N} f_s t\right) \quad (1)$$

where

$$b_n = \frac{2}{(2n-1)\pi} \sin\left(\frac{(2n-1)\pi}{N}\right). \quad (2)$$

In (1), the term $1/N$ represents a constant that leads to an attenuation of the integrator's output at node v_x , which is the desirable effect of the PNIS scheme to reduce the capacitance spread. The other terms, which represent tones at frequencies $[(2n-1)/N]f_s$, generate spurs (i.e., alias components) in the lossy integrator. As n increases, the magnitude of b_n decreases, as well as the power of the spurious tones generated. Furthermore, the terms with $n > (N+1)/2$ have frequencies that are beyond f_s and their impact is significantly reduced by the anti-alias filter preceding the SC filter. To limit the number of

¹The results can be generalized to the case where $m \neq 1$, and the secondary clock θ is active during m consecutive clock periods of the master clock ϕ and inactive during the remaining $N-m$ periods. In this case, the following Fourier series expansion should be considered:

$$P(t) = \frac{m}{N} + \sum_{n=1}^{\infty} \frac{2}{(2n-1)\pi} \sin\left(\frac{m(2n-1)\pi}{N}\right) \cos\left(\frac{2(2n-1)\pi f_s}{N} t\right).$$

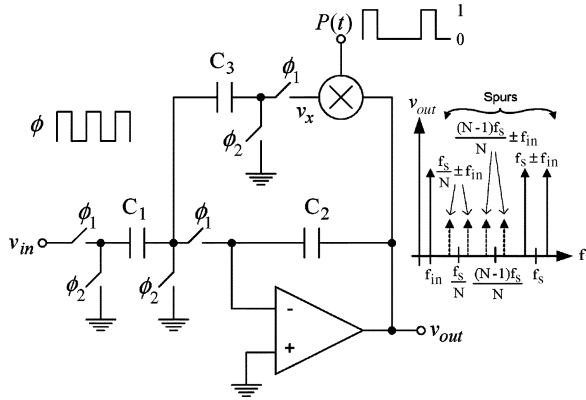


Fig. 2. Equivalent representation of a SC lossy integrator operating with PNIS.

terms that fall within the Nyquist band of the main clock $0 \leq f \leq f_s/2$ to only $n = 1$, $N \leq 4$ must be chosen. Nevertheless, alias components due to b_1 fall inevitably within this band and therefore an evaluation of their power is mandatory in the design.

Assuming a continuous-time sinusoidal waveform $v_{in}(t) = Ae^{\pm j2\pi f_{in}t}$ applied at the input terminal of the SC integrator, it is expected that the integrator's output will have several tones generated by the sampling of the signal (considered ideal in this analysis) and the use of the slower clocks. It is therefore reasonable to expect that in a first approximation, the output signal has several frequency components that can be expressed as

$$v_{out} \cong H_1 A \left(e^{\pm j2\pi f_{in}t} + e^{\pm j2\pi (f_s \pm f_{in})t} \right) + H_2 A \left(e^{\pm j2\pi (f_s/N \pm f_{in})t} + e^{\pm j2\pi (f_s(N-1)/N \pm f_{in})t} \right). \quad (3)$$

The first term in (3) represents the output component at the original input frequency that leads to the ideal integrator's transfer function. Due to the sampled nature of SC circuits, alias components appear at the output at $f = f_s \pm f_{in}$, as depicted in Fig. 2 and represented by the second term in (3). Although ideal sampling of a continuous-time signal would result in a spectrum with replicas at integer multiples of f_s with the same magnitude (as stated in (3)), in practice the sample-and-hold operation in SC circuits, the finite conductance of the switches, and the speed of the amplifiers partially reduce the amplitude of these replicas. Therefore, (3) leads to an upper bound in the alias estimation. The third and fourth terms in (3) represent the alias components or spurious tones due to b_1 (dashed lines in the frequency spectrum shown in Fig. 2).

Analysis of the lossy SC integrator using charge re-distribution techniques and assuming that $b_n = 0$, leads to the following expression for the integrator's transfer function (ratio of the fundamental tone at the output and the input tone), which corresponds to H_1 in (3)

$$H_1 = H(f) = - \left(\frac{C_1}{C_2 + \frac{C_3}{N}} \right) \cdot \left(\frac{1}{1 - \frac{C_2}{C_2 + C_3/N} e^{-j(\frac{2\pi f}{f_s})}} \right). \quad (4)$$

The advantage of using PNIS is evident in this expression, since the effective value of C_3 is reduced by a factor N . To obtain the magnitude of the alias due to PNIS, notice first that the transfer function from a signal applied at node v_x to v_{out} is an integrator given by

$$G(f) = v_{out}(f)/v_x(f) = (C_3/C_1)H(f). \quad (5)$$

On the other hand the mixing of the term $b_1 \cos(2\pi(f_s/N)t)$ in (1) with the integrator's output (taking into account the fundamental tone at f_{in} and the alias at $f_s \pm f_{in}$ due to the master clock) leads to the spurious tones at v_x generated by PNIS that can be expressed as

$$v_x = \left(\frac{b_1}{2} \right) H(f_{in}) \left(Ae^{\pm j2\pi(\frac{f_s}{N} \pm f_{in})t} + Ae^{\pm j2\pi(\frac{(N-1)f_s}{N} \pm f_{in})t} \right). \quad (6)$$

Therefore, from (3)–(6), it can be obtained that

$$H_2 = \left(\frac{b_1 C_3}{2 C_1} \right) H(f_{in}) H \left(\frac{f_s}{N} \pm f_{in} \right) \quad (7)$$

where $H((f_s/N) \pm f_{in}) = H(((N-1)f_s/N) \pm f_{in})$.

For $N \geq 3$, the ratio between the magnitude of the alias components due to PNIS and the fundamental tone at the output of the integrator is then given by

$$\left| \frac{v_{out} \left(\frac{f_s}{N} \pm f_{in} \right)}{v_{out}(f_{in})} \right| = \left(\frac{b_1 C_3}{2 C_1} \right) \left| H \left(\frac{f_s}{N} \pm f_{in} \right) \right| \quad (8a)$$

$$\left| \frac{v_{out} \left(\frac{(N-1)f_s}{N} \pm f_{in} \right)}{v_{out}(f_{in})} \right| = \left(\frac{b_1 C_3}{2 C_1} \right) \left| H \left(\frac{(N-1)f_s}{N} \pm f_{in} \right) \right|. \quad (8b)$$

For $N = 2$ the ratio of the alias to the fundamental component is computed as

$$\left| \frac{v_{out} \left(\frac{f_s}{N} \pm f_{in} \right)}{v_{out}(f_{in})} \right| = \left(b_1 \frac{C_3}{C_1} \right) \left| H \left(\frac{f_s}{N} \pm f_{in} \right) \right|. \quad (9)$$

Repeating the analysis for the biquadratic filter of Fig. 1, it can be found that (3) and (5)–(9) are still valid if $H(f)$ is replaced by the proper filter's transfer function; this case is considered in the following section.

An additional effect is the clock feedthrough at f_s/N due to the secondary clock. Since the clock feedthrough is injected at node v_x , (5) must be used to estimate its magnitude at the output of the filter. However, it can be noticed that since the frequency of the additional clock feedthrough is always outside

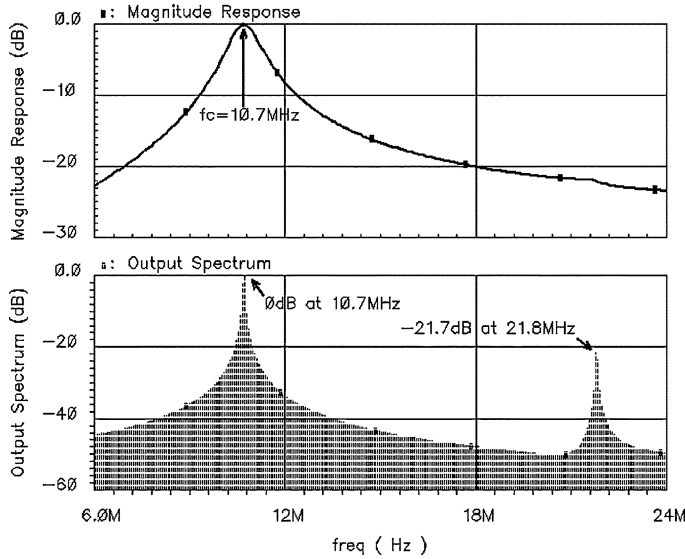


Fig. 3. Simulated frequency response and output spectrum of the bandpass filter. Top trace corresponds to filter's frequency response and bottom trace corresponds to filter's output spectrum for an input tone at filter's center frequency.

the filter's passband, it is drastically attenuated in high- Q filter applications.

III. SIMULATION RESULTS

For the verification of the analytical results, a 10.7-MHz second-order SC bandpass filter with unity peak gain, $Q = 10$, $f_s = 65$ MHz, $m = 1$ and $N = 2$ was designed and simulated using a 0.35- μm CMOS technology; the technology files were provided by MOSIS through its MEP program. The capacitor ratios were $C_4/C_2 = 1$, $C_4/C_3 = 5$, and $C_3/C_1 = 2$; the actual Q is determined by $N \cdot C_4/C_3$ (10 in this case). The magnitude of the frequency response $|H(f)| = v_{\text{out}}(f)/v_{\text{in}}(f)$ is shown in the top trace of Fig. 3. In the bottom trace, the output spectrum due to a 10.7-MHz sinusoidal input signal, normalized to the magnitude of the input signal, is also shown. The ratio between the power of the alias tone at $f_{\text{spur}} = f_s/2 - f_{\text{in}} = (65/2 - 10.7)$ MHz = 21.8 MHz generated at the output of the filter and the power of tone at $f_{\text{in}} = 10.7$ MHz, obtained through circuit simulations, is -21.7 dB. For $N = 2$, $C_3/C_1 = 2$ and magnitude response at f_{spur} of -22 dB (see Fig. 3), (9) predicts a ratio of the tones of -20 dB, which is relatively close to the simulated value.

Extensive simulations have been carried out for different frequencies; the results are shown in Fig. 4. Fig. 4(a) shows the ratio of the alias tone at $f_s/2 - f_{\text{in}}$ and the amplitude of the input tone, and compares with the results predicted by (7); the two peaks in this plot are the result of the multiplication of the transfer functions, one of them shifted by f_s/N Hz. The ratios between such alias tones and the fundamental tone at the output of the filter predicted by (9) and those obtained through circuit simulations, are shown in Fig. 4(b). Notice that these latter plots are a mirrored version of the filter's frequency response (shown in Fig. 3) but scaled by $b_1 C_3/C_1$, and shifted by f_s/N Hz, as expected from (9). The error in the estimation is less than 2.5 dB for all frequencies, and as aforementioned, this is an upper bound prediction of the alias components.

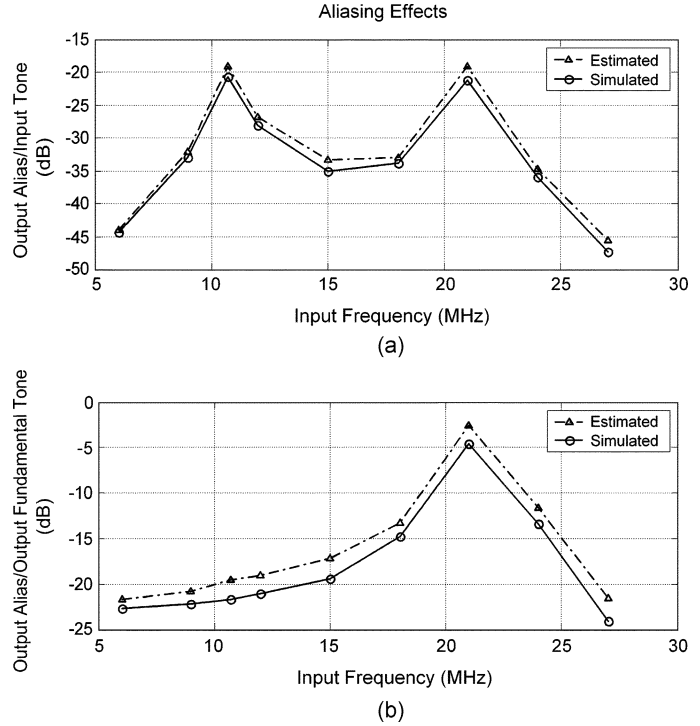


Fig. 4. Simulated versus predicted aliasing effects at the output of the filter. (a) Power of the alias component at the output of the filter relative to the input tone power. (b) Power of alias component at the output of the filter relative to the power of fundamental tone at the output.

IV. IMPLICATIONS OF PNIS ON THE DESIGN OF IF FILTERS

The use of periodical nonuniform individual sampling for the design of IF filters results in additional image sidebands. For $N \leq 4$, the most important sidebands are located at $f_{\text{sb}} = (f_s/N) \pm f_c$ and $f_{\text{sb}} = ((N-1)f_s/N) \pm f_c$, where f_c is the filter's center frequency. From (8) and (9), for the same power level of the signal at the filter's center frequency and the interferer at f_{sb} , the ratio between the magnitude of the in-band alias component and that of the desired signal at f_c is given by

$$\frac{\text{in-band alias}}{\text{desired}} = b_1 \frac{C_3}{C_1} |H(f_{\text{sb}})| \text{ when } N = 2 \quad (10a)$$

$$\frac{\text{in-band alias}}{\text{desired}} = \frac{b_1}{2} \frac{C_3}{C_1} |H(f_{\text{sb}})| \text{ when } N \geq 3. \quad (10b)$$

These equations represent the filter's image rejection (IR) function due to the use of PNIS; notice that the larger the peak gain given by $N \cdot C_1/C_3$, the larger the image rejection. Similarly, high- Q filters present better image rejection figures.

For the case of the design example discussed in Section III ($N = 2$), according to (10) an interferer at $f_{\text{sb}} = 21.8$ MHz generates an in-band alias component at $f_c = 10.7$ MHz whose magnitude is -20 dBc; these IR figures may not be enough in many practical cases. Obviously, it is desirable to suppress as much as possible the out-of band interferers prior to the filter section that uses slower clocks.

Let us extend the analysis to higher order filters by cascading second-order sections and possibly a first-order section for the case of odd-order filters. The general case is shown in Fig. 5. The output power of a tone in the stop-band of the filter at f_{sb} is attenuated by the overall filter's transfer function $H_{\text{overall}}(f_{\text{sb}}) =$

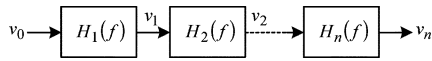


Fig. 5. Higher order cascaded filter.

$H_1(f_{sb}) \cdots H_n(f_{sb})$ which will typically offer high rejection as the number of stages increases. Hence, it is the first stage that uses PNIS the one that determines the rejection of the images produced by the sidebands located around f_{sb} . That stage will generate in-band alias signals that will not be filtered by subsequent stages. Therefore, in the design of IF filters using PNIS, the following design guidelines should be followed.

- 1) Once f_s is defined, choose N such that possible strong interferers do not fall at or close to the critical frequencies around f_{sb} . To reduce the number of sidebands present within the passband of the anti-alias filter due to PNIS, to maintain $N \leq 4$ is advisable.
- 2) Place the low- Q resonators as the first stages of the design, which do not require the use of slower clocks. Usually, low- Q sections do not demand high-capacitor ratios and each biquadratic bandpass section provides attenuation of 6 dB/octave for the signals around f_{sb} . In addition, the continuous-time anti-alias filter helps attenuating further the power of the signals at the critical frequencies without generating in-band spurs. Thus, PNIS techniques can be used for the implementation of the most demanding high- Q sections as the latter stages, to further attenuate the channels near to the passband of the desired channel.
- 3) If using PNIS for the first stage, it must provide the required attenuation at f_{sb} as given by (10). Be sure that the signal to alias interferer ratio is good enough for the application. If additional rejection is required, the anti-alias filter preceding the SC IF filter must provide the additional attenuation at f_{sb} .
- 4) Similar recommendations apply to low-pass filters.

V. CONCLUSION

An equivalent model for the analysis of alias components due to periodical nonuniform individual sampling in SC filters has been presented. Practical expressions to estimate the power of such alias components at the output have been obtained and verified through circuit simulation in the context of a lossy integrator and a second-order SC section. The theoretical results were then extended to cascaded higher order filters, and design guidelines for the implementation of intermediate frequency filters have been provided.

REFERENCES

- [1] J. Adut, J. Silva-Martinez, and M. Rocha-Perez, "A 58-dB SNR sixth-order broadband 10.7-MHz SC ladder filter," in *Proc. IEEE Custom Integr. Circuits Conf.*, Sep. 2003, pp. 13–16.
- [2] W. Sansen and P. Van Peteghem, "An area-efficient approach to the design of very large time-constants in switched-capacitor integrators," *IEEE J. Solid-State Circuits*, vol. SC-19, no. 10, pp. 772–779, Oct. 1984.
- [3] K. Nagaraj, "A parasitic-insensitive area-efficient approach to realizing very large time constants in switched-capacitor circuits," *IEEE Trans. Circuits Syst.*, vol. 36, no. 9, pp. 1210–1216, Sep. 1989.
- [4] J. L. Ausin *et al.*, "Switched-capacitor circuits with periodical nonuniform individual sampling," *IEEE Trans. Circuits Syst. II, Analog Digit. Signal Process.*, vol. 50, no. 8, pp. 404–414, Aug. 2003.
- [5] K. W. H. Ng, V. S. L. Cheung, and H. C. Luong, "A 44-MHz wideband switched-capacitor bandpass filter using double-sampling pseudo-two-path techniques," *IEEE J. Solid-State Circuits*, vol. 40, no. 3, pp. 781–784, Mar. 2005.
- [6] K. A. Ng and P. K. Chan, "A time-multiplexed switched-capacitor CDS equalizer with reduced crosstalk layout," *IEEE Trans. Circuits Syst. I, Reg. Papers*, vol. 52, no. 10, pp. 2065–2074, Oct. 2005.
- [7] P. J. Hurst, "Shifting the frequency response of switched-capacitor filters by nonuniform sampling," *IEEE Trans. Circuits Syst.*, vol. 38, no. 1, pp. 12–19, Jan. 1991.
- [8] M. B. Ghaderi, J. A. Nossek, and G. Temes, "Narrow-band switched-capacitor bandpass filters," *IEEE Trans. Circuits Syst.*, vol. CAS-29, no. 8, pp. 557–572, Aug. 1982.
- [9] P. J. Quinn, K. Hartingsveldt, and A. van Roermund, "A 10.7-MHz CMOS SC radio IF filter using orthogonal hardware modulation," *IEEE J. Solid-State Circuits*, vol. 35, no. 12, pp. 1865–1876, Dec. 2000.